RSC Advances

PAPER

View Article Online
View Journal | View Issue

Cite this: *RSC Adv.*, 2025, **15**, 36504

Changes in tea exosome-like nanoparticles fermented by *Aspergillus cristatus* and the preventive effects on non-alcoholic fatty liver disease

Meiling Guo,†[a] Chengwu Song,†[abc] Jing Tang,†[d] Yiping Li,[a] Zhaoxiang Zeng,[a] Xiaoliu Hu,[a] Xin Huang,[e] Sha Wei,[e] Cheng Chen,[a] Yinping Tang,*[a] Rongzeng Huang*[ac] and Shuna Jin *[ce]

Research on dark tea-derived exosome-like nanoparticles (TELNs) and microbial fermentation-mediated modifications of TELNs remains limited. To comprehensively explore the fermentation-induced alterations in TELNs' physical properties, metabolic composition, and biological functions, a systematic investigation was conducted in this study. Particle size distribution, zeta potential, protein content, and particle concentration of TELNs were characterized and compared before and after *Aspergillus cristatus* (AC) fermentation using nanoparticle tracking analysis (NTA), dynamic light scattering (DLS), and bicinchoninic acid assay (BCA), respectively. Untargeted metabolomics was employed to profile metabolic changes, while functional assessment was performed in a non-alcoholic fatty liver disease (NAFLD) mouse model. As a result, AC fermentation significantly reduced the particle size of TELNs and increased their yield. It altered the overall metabolite profile of TELNs, and a total of 30 differential metabolites were tentatively identified, mainly including flavonoids, alkaloids, and lipids. Meanwhile, AC fermentation enhanced the blood-lipid-lowering and anti-inflammatory abilities of TELNs in NAFLD mice. This study deepened the understanding of the molecular-level changes during tea fermentation, and offered a new perspective on the applications of dark tea or TELNs in the fields of food science and medical healthcare.

Received 30th April 2025
Accepted 15th September 2025

DOI: 10.1039/d5ra03044g

rsc.li/rsc-advances

1. Introduction

In recent years, nanomedicine delivery systems have emerged as a promising therapeutic strategy, garnering significant attention from the medical research community due to their excellent biocompatibility, superior targeting capability, and minimal toxicity.[1–3] Among these, plant-derived exosome-like nanoparticles (PELNs) represent a class of green, nano-scale vesicles isolated from plant sources.[4] As crucial mediators of intercellular communication, PELNs have been shown to carry diverse bioactive molecules including lipids, proteins, nucleic acids, and various metabolites, which can modulate physiological functions in recipient cells.[5,6] For example, studies revealed that Tangerine-peel-derived exosome-like nanovesicles possessed the capacity to regulate glucose and lipid metabolism.[7] Similarly, grapefruit-derived nanovesicles were demonstrated to ameliorate colitis in mice by suppressing proinflammatory cytokine production.[8] Furthermore, exosomes isolated from *Artemisia capillaris* have been proven effective in reversing both hepatic lipid accumulation and inflammatory damage in NAFLD mice.[6] These collective findings highlight the significant therapeutic potential of PELNs as natural and highly effective therapeutic agents.

Tea (*Camellia sinensis* L.), one of the world's three major beverages, is widely consumed globally.[9] As a post-fermented tea, dark tea attracts considerable attention in food science and medical research due to its unique fermentation process and abundant bioactive compounds.[10,11] The fermentation of dark tea has been reported to be primarily mediated by microorganisms, and *Aspergillus cristatus* (AC) is one of the predominant fungal species involved in the biotransformation of various compounds.[12] Recent studies have demonstrated that dark tea exhibited significant effects on regulating lipid metabolism, improving insulin resistance, and attenuating inflammatory responses, suggesting its potential application in the prevention and treatment of metabolic disorders.[13,14] Our

[a]*School of Pharmacy, Hubei University of Chinese Medicine, Wuhan 430065, Hubei, China. E-mail: yptang@hbucm.edu.cn; rongzenghuang_2018@hbucm.edu.cn*

[b]*Center of Traditional Chinese Medicine Modernization for Liver Diseases, Hubei University of Chinese Medicine, Wuhan 430065, Hubei, China*

[c]*Hubei Shizhen Laboratory, Wuhan 430061, Hubei, China. E-mail: jinshuna2021@hbucm.edu.cn*

[d]*Wuhan Petrochemical Hospital, Wuhan 430082, Hubei, China*

[e]*School of Basic Medical Sciences, Hubei University of Chinese Medicine, Wuhan 430065, Hubei, China*

† These authors contributed equally to this work.

preliminary studies also have demonstrated that Fuzhuan brick tea could ameliorate glucolipid metabolic disorders.[15,16] In addition, it was found that the activity of tea leaves was significantly enhanced after AC fermentation.[17] These findings have indicated that dark tea possesses the activity of regulating glucose and lipid metabolism, and the microbial-mediated fermentation process may have played a crucial role in potentiating its biological function.

During dark tea processing, fermentation was identified as the pivotal technological step that determined final product quality.[18] This critical process not only significantly altered the color, aroma, and flavor characteristics of tea leaves, but also profoundly modified their nutritional composition while inducing complex cellular physiological changes.[19] Amidst this series of changes, the secretion level, compositional components, and functional characteristics of tea-derived exosome-like nanoparticles (TELNs) might undergo significant alterations. Researchers had successfully isolated natural nanoparticles from both fresh tea leaf homogenates and infusions of green tea, white tea, and black tea.[5,20–22] Studies have shown that the average diameter of these nanoparticles ranges from 50 to 400 nanometers. They carried a negative charge on their surface and were mainly composed of components such as proteins, lipids, RNA, and metabolites, demonstrating good biological activity. Notably, as the aging time prolonged, the particle size of the nanoparticles in white tea infusions exhibited a decreasing trend, and their yield decreased gradually as well.[21] Moreover, TELNs isolated from fresh tea leaf homogenates have been proven to be capable of improving lipid metabolism and inhibiting the expression of cellular pro-inflammatory factors.[3,23] Similarly, the colloidal nanoparticles (NPs) in black tea infusions also exhibited significant antioxidant activity.[24] However, numerous knowledge gaps still exist in the current field of TELNs. To be more precise, the studies regarding TELNs sourced from dark tea and the influence of AC fermentation on the alterations of TELNs have yet to reach definite conclusions.

Therefore, in the present study, size-exclusion chromatography (SEC) was employed to isolate TELNs from fermented and unfermented tea leaves, respectively. A systematic comparison was conducted to evaluate alterations in particle size distribution, surface potential, protein concentration, and particle number of TELNs before and after tea fermentation. The metabolic profiles of TELNs were subsequently analyzed by untargeted metabolomics using ultra-performance liquid chromatography coupled with quadrupole time-of-flight mass spectrometry (UPLC-QTOF-MS/MS) to reveal the differences in TELNs before and after fermentation. In addition, to investigate the impact of fermentation on the functional characteristics of TELNs, a NAFLD mouse model was utilized to assess comparatively the biological effects of TELNs before and after fermentation.

2. Materials and methods

2.1 Materials and reagents

HPLC-grade methanol was purchased from Fisher Scientific (Fair Lawn, NJ, USA). Analytical grade formic acid (≥98%) was sourced from Sinopharm Chemical Reagent Co., Ltd., Shanghai, China. The fexofenadine reference standard was supplied by the National Institute for Food and Drug Control. Deionized water was prepared using a Milli-Q water system (Millipore, Bedford, MA, USA). qEVsingle-gen-2 chromatographic columns were obtained from Izon Science. PBS (Phosphate-Buffered Saline, pH 7.4) was acquired from ServiceBio (Wuhan, China). Phosphotungstic acid (5%) was sourced from Yuanye Bio (Shanghai, China). Pure carbon support film (300 mesh) was purchased from Beijing Zhongjing Technology Co., Ltd. BCA Protein Assay Kit was procured from Beyotime Biotech Inc and the assay kits for TC (total cholesterol, 20241210), TG (triglyceride, 20250321), HDL-C (high-density lipoprotein cholesterol, 20250102), and LDL-C (low-density lipoprotein cholesterol, 20250103) were obtained from Nanjing Jiancheng Bioengineering Institute (Nanjing, China). ALT (Alanine Aminotransferase, Cat No. E-BC-K236-M) and AST (Aspartate Aminotransferase, Cat No. E-BC-K235-M) assay kits were provided by Elabscience. The IL-6 (Interleukin-6, A20650525) and TNF-α (Tumor Necrosis Factor-α, A28250554) ELISA kits were purchased from Hangzhou Multi Sciences Biotech Co., Ltd.

Sun-dried tea-leaves were collected in November 2021 from Xianning City, Hubei Province, China. The tea-derived fungal strain AC was isolated from Fuzhuan Brick-Tea samples obtained in previous research.[12]

2.2 Fermentation of tea leaves

The spore suspension of AC was adjusted to approximately 10^6 CFU mL^{-1}. Sun-dried tea leaves (35 g) with a moisture content of 10.06% were sterilized at 121 °C for 20 min. After sterilization, the samples were mixed with spore suspensions of AC to produce a solid content of ~67% (w/w) for fermentation.[12] As a control, the unfermented tea leaves were treated with sterile distilled water instead of the spore suspension. Samples were fermented in a constant temperature and humidity incubator (HWS-150B, 30 °C, 50% RH) for 10 days. Tea samples were collected at different fermentation times (0 days and 10 days) and stored in sterile polyethylene bags that were placed at −20 °C until further processing. Seven parallel samples were prepared for each group to ensure validity and repeatability.

2.3 TELNs isolation

Tea samples (5.0 g) were extracted in boiling water bath (100 °C) for 30 min with 50 mL of boiling Milli-Q water.[22,25] The tea powder was subsequently filtered, and the filtrate was concentrated to a final volume of 10 mL. The obtained tea soup samples were sequentially centrifuged at 1000 g for 20 min, 5000 g for 40 min to remove large plant debris. Followed at 10 000 g for 60 min to remove small cell debris, the whole process was carried out at 4 °C.[3] The obtained supernatant of 150 μL was added into the qEV column, which had been balanced with sterile PBS solution at room temperature for 30 min. A micro injection pump was connected above to continuously output sterile PBS at room temperature for elution, and calculated the number of drops below the chromatographic column.

The eluate was collected in two-drop segments and analyzed for particle size, zeta potential, and morphological characteristics. According to the tracked total protein detection results, the first 14 drops were identified as the column's dead volume, whereas drops 15 to 24 comprised the TELNs fraction and what followed was the part about proteins. TELNs isolated from tea leaves at 0 days (unfermented), 10 days (unfermented), and 10 days (AC-fermented) were categorized into the UF0, UF10, and AC10 groups, respectively. Subsequently, the TELNs were collected and stored at −80 °C for further use.

2.4 Physical characterization of TELNs

The particle Size distribution and concentration of TELNs were measured using the Nanoparticles Tracking Analysis instrument (NTA, Zetaview-PMX120-Z, Particle Metrix, Meerbusch, Germany) with the corresponding software ZetaView (version 8.05.14 SP7). In the NTA detection, samples were diluted with PBS filtered through a 0.22 μm filter to reach optimal concentrations (10^6–10^7 particles per mL) prior to measurement. Eleven positional measurements were recorded following calibration with 100 nm polystyrene standards, with ambient temperature maintained at 23–30 °C. For zeta potential analysis, TELNs of 200 μL was mixed with 1 mL deionized water and vortexed before measurement using a Zetasizer Nano ZS90 (Malvern). Transmission electron microscopy (TEM) sample preparation involved deposition of 5 μL samples onto pure carbon support membrane, followed by 10 min adsorption. Excess fluid was blotted and grids were negatively stained with 5% phosphotungstic acid for 3 min. Morphological examination was conducted using a JEM-1400, JEOL at 80 kV acceleration voltage. In addition, total protein content was quantified using the BCA assay according to manufacturer specifications.

2.5 Sample preparation for untargeted metabolomics

TELNs samples stored at −80 °C were thawed at room temperature. 100 μL of sample was extracted with 400 μL of methanol solution containing fexofenadine as the internal standard at a final concentration of 100 ng mL^{-1}. After vortexed for 2 min, ultrasonically extracted for 15 min, and finally centrifuged at 12 000 rpm for 15 min at 4 °C. 400 μL of the supernatant was took to blow dry with nitrogen and redissolved with 100 μL of 90% methanol. Repeated the above extraction process and then transferred the supernatant into the sample vials. Aliquots of all supernatant samples were mixed to make a pooled sample, which served as the quality control (QC) sample.

2.6 UPLC-QTOF-MS/MS conditions and parameters

Chromatographic separations were performed at an ACQUITY UPLC M-Class system (Waters, Mass. USA) equipped with a ACQUITY UPLC BEH C18 column (2.1 × 100 mm, 1.7 μm). The column temperature was 40 °C, the flow rate was 0.3 mL min^{-1} and the sample injection volume was 2.0 μL. Mobile phases A and B were water/formic acid (1000 : 1, v/v) and methanol respectively. The gradient elution procedures were as follows: 0 min, 10% B; 15.0 min, 95% B; 20.0 min, 95% B; 21.0 min, 10% B; 25.0 min, 10% B.

Mass spectrometric analyses were carried out using a Waters Xevo G2-XS QTOF system equipped with an electrospray ionization source (Waters, Mass, USA). Positive and negative ion electrospray data acquisition was performed in the sensitivity analysis mode, which was used for metabolomics analysis and structural determination respectively. The operational parameters were as follows: cone gas flow rate and the desolvation gas flow rate, 50 L h^{-1}; ion source temperature, 100 °C; desolvation gas temperature, 500 °C; capillary voltage, 3 kV; cone voltage, 20 V; primary collision energy, 10 eV; secondary collision energy, 35 eV. In the MS^E mode, the mass spectrometry range of the full scan was between *m/z* 50 to 1500 within 1.0 s.

2.7 Animals and treatment

Forty male C57BL/6J mice with 8 weeks old (22–24 g) were obtained from Hunan Slack Jingda Laboratory Animal Co., Ltd [License: SCXK (Xiang) 2021-0002]. The mice were housed in an animal room with a temperature of 24 ± 2 °C and a humidity of 60% ± 5%. The light/dark cycle was set to 12/12 hours. After a 5-day adaptation period, the mice were randomly divided into the following five groups of 8 each: Normal group (N group), NAFLD model group (M group), Positive control group (P group), UF0 treatment group (UF group) and AC10 treatment group (AC group). The N group was fed a standard diet, while the model group and the treatment groups were fed a high-fat diet. The basal diet was commercially obtained from Medicience Biopharmaceutical Co., Ltd (Jiangsu, China). The high-fat diet (HFD) was formulated with the following composition (w/w): 67.8% basal diet, 15% egg yolk powder, 15% lard, 2% cholesterol, and 0.2% sodium cholate. Body weights were recorded three times weekly throughout the study period, while food and water intake were monitored daily.

Following a 2-week model induction period, mice in the N and M groups received 0.2 mL PBS *via* daily oral gavage. The remaining three treatment groups were administered their respective interventions: the P group was treated with simvastatin (40 mg per kg per day), while UF and AC groups received either unfermented TELNs or AC-fermented TELNs at a dose of 0.2 mL per day. All treatments were maintained for 4 consecutive weeks.

After the four-week intervention period, the mice were anesthetized with sodium pentobarbital administered *via* intraperitoneal injection, sacrificed by cervical dislocation, and subsequently, blood and liver samples were collected. Blood samples were centrifuged at 12 000 rpm for 10 minat 4 °C to obtain serum and then stored at −80 °C until analysis. Liver tissues were fixed and stained with oil red O for histological examination. The levels of serum TC, TG, HDL-C, LDL-C, ALT, AST, IL-6 and TNF-α were determined by the enzyme-colorimetric method according to the instructions of the kit using a microplate reader. The atherosclerosis index (AI) was calculated according to the following formula: AI = (TC-HDL-C)/HDL-C.[26] All animal experimental procedures were given permission by the Institutional Animal Care and Use

Committee of Hubei University of Chinese Medicine (HUCMS 78475747).

2.8 Data analysis

The software MassLynx v4.1 (waters, Milford, MA, USA) was used to obtain the raw data from UPLC-QTOF-MS/MS. The open-access software MS-DIAL (Version 4.9) was employed to conduct comprehensive data processing tasks, including peak detection, peak alignment, spectral deconvolution, identification, and normalization.[27] Detailed parameter settings were provided in the SI.

Principal component analysis (PCA) and orthogonal partial least squares-discriminant analysis (OPLS-DA) were performed utilizing SIMCA 14.1 software (Umetrics AB, Umeå, Sweden). Data visualization was conducted using Origin 2021 (OriginLab Corporation, Northampton, MA, USA) and GraphPad Prism 8.0 (GraphPad Software Inc). Statistical analyses were carried out with SPSS version 26.0 (SPSS, Inc., Chicago, IL, USA). Qualitative analysis of metabolites was achieved by matching their fragmentation masses against the Human Metabolome Database (**https://www.hmdb.ca**) and relevant literature. Quantitative analysis was performed using Quanlynx software V4.1 (Waters). Correlation analysis was conducted in Cytoscape_v3.9.1, with a p-value <0.05 considered statistically significant.

3. Results

3.1 Characterization of TELNs

As shown in Fig. 1, TELNs were isolated from tea infusions through sequential differential centrifugation followed by size-exclusion chromatography. TEM analysis showed that the extracted nanoparticles exhibited a nearly spherical morphology with a double-layer membrane and an average diameter of 100 nm, consistent with the characteristics of previously reported PELNs.

To explore the changes in TELNs before and after AC fermentation, a comprehensive comparison of the physical properties among the UF0, UF10 and AC10 groups was conducted. Size distribution and concentration of TELNs were analyzed by NTA, during which the Brownian motion state of particles in solution was recorded (Fig. 2a–c). The nanovesicles exhibited a relatively uniform peak distribution, suggesting high purity of the isolated TELNs.[28] Mean particle sizes of TELNs were determined to be 134.47 ± 5.18 nm, 129.44 ± 3.83 nm and 127.00 ± 6.09 nm for UF0, UF10 and AC10 respectively (Fig. 2d). Notably, TELNs in the AC10 group were significantly smaller than those in the UF0 group. Zeta potential measurements revealed surface charges of TELNs in the UF0, UF10 and AC10 groups were −15.00 ± 1.45 mV, −15.63 ± 0.79 mV and −15.45 ± 1.23 mV respectively. This finding indicated that all groups carried a consistent negative charge without significant variation (Fig. 2e). TELNs concentration was assessed based on protein content and particle count. Protein contents were measured as 0.17 ± 0.01 mg mL^{-1} (UF0), 0.22 ± 0.03 mg mL^{-1} (UF10), and 0.17 ± 0.01 mg mL^{-1} (AC10) (Fig. 2f). Meanwhile, the particle numbers were quantified as (2.87 ± 0.35) $\times 10^{10}$ particles per mL, (5.84 ± 1.41) $\times 10^{10}$ particles per mL and (4.11 ± 0.46) $\times 10^{10}$ particles per mL respectively (Fig. 2g). Surprisingly, quantitative analysis revealed that the UF10 control group demonstrated significantly higher vesicle concentrations than the other two groups. Furthermore, the AC10 group exhibited a markedly greater particle count relative to UF0 ($p < 0.05$). The above results indicated that AC fermentation induced substantial modifications in TELNs physical characteristics, manifesting as both reduced particle diameter and enhanced secretory output.

3.2 Untargeted metabolomic analysis

To determine whether fermentation altered TELNs composition, untargeted metabolomics was performed on UF0, UF10, and AC10 samples. As demonstrated in Fig. S1, initial analysis employed an unsupervised PCA model to assess global metabolite differences among groups, with QC samples incorporated into the analysis. The PCA results revealed three key findings:

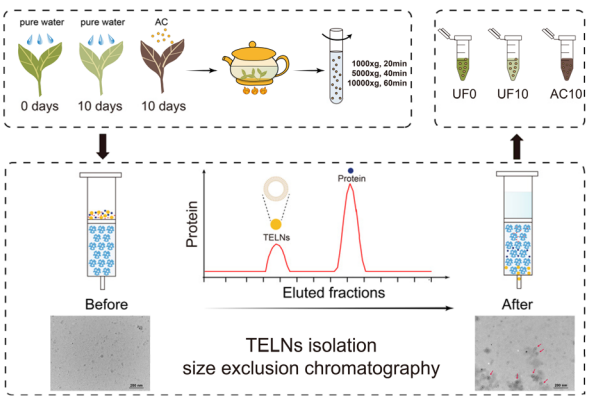

Fig. 1 The TELNs isolated from tea leaves at 0 days (unfermented), 10 days (unfermented), and 10 days (AC-fermented), respectively. AC, *Aspergillus cristatus*. Red arrows indicate the representative TELNs.

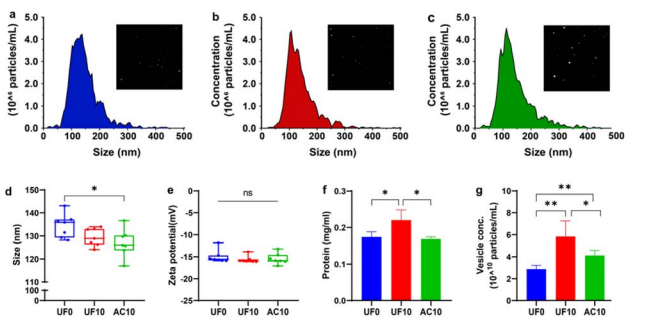

Fig. 2 Characterization of TELNs before and after tea fermentation. (a–c) Representative size distribution profiles and Brownian motion state of TELNs in the UF0 group (a), UF10 group (b) and AC10 group (c). (d–g) Comparison of (d) average size, (e) Zeta potential, (f) protein yield and (g) Vesicle concentration. "UF0", "UF10", and "AC10" represent the TELNs isolated from tea leaves at 0 days (unfermented), 10 days (unfermented), and 10 days (AC-fermented), respectively. AC, *Aspergillus cristatus*. All values are expressed as mean ± SD (*$p < 0.05$, **$p <$ 0.01, ns: not significant; $n = 7$).

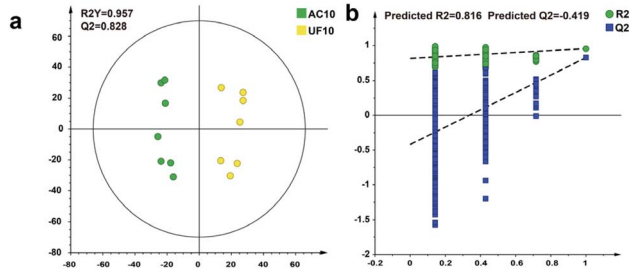

Fig. 3 (a) OPLS-DA analysis of the UF10 and AC10 groups (b) 999 permutation validation results of the UF10 and AC10 groups "UF0", "UF10", and "AC10" represent the TELNs isolated from tea leaves at 0 days (unfermented), 10 days (unfermented), and 10 days (AC-fermented), respectively. AC, *Aspergillus cristatu*.

(1) the tight clustering of QC samples demonstrated the excellent instrument stability and reproducibility during LC-MS analysis; (2) distinct intra-group clustering trend were observed of all experimental samples indicated the good repeatability of TELNs preparations; (3) although UF0 and UF10 displayed partial overlap, clear separation between UF and AC groups was observed, indicating substantial modification of TELNs metabolite profiles induced by AC fermentation. To specifically elucidate the effects attributable solely to fermentation, OPLS-DA analysis was conducted comparing UF10 and AC10 groups. As shown in Fig. 3a, the values of $R2Y = 0.957$ and $Q2 = 0.828$ indicated that the model had good fitting and applicability. Moreover, 999 permutation tests confirmed the validity of the model with the predicted $R2 = 0.816$ and $Q2 = -0.419$, both of which were lower than those of the real model, reflecting that the OPLS-DA model was not over-fitting (Fig. 3b).

The raw UPLC-QTOF-MS/MS data were processed by means of MS-DIAL software, thereby generating a dataset of 2104 metabolic features. Feature selection was then executed based on the OPLS-DA model for the UF10 and AC10 groups. By applying thresholds of variable importance in projection (VIP) > 1.0 and fold change (FC) > 1.1 or <0.9, 737 qualified features were obtained for subsequent analysis. Afterwards, metabolite identification was accomplished through the matching of precursor ion peaks and MS/MS fragments against online databases, which led to the annotation of 69 compounds. These candidate metabolites were then quantitatively analyzed across all three experimental groups. To explore the differences, comparative analysis was carried out between UF10 and AC10, as well as between UF0 and AC10, with the utilization of the

Table 1 The *p*-values and fold changes of 30 differential metabolites between the unfermented and fermented group[a]

			AC10/UF10		AC10/UF0	
No.	Metabolites	VIP	*p*-Value	FC	*p*-Value	FC
M1	Caffeine	1.26	0.009	1.44	0.002	1.84
M2	Prunin 6″-*O*-gallate	1.67	0.002	0.05	0.002	0.05
M3	Epicatechin 3-*O*-gallate	1.58	0.002	0.02	0.002	0.03
M4	Epicatechin 3-*O*-(4-methylgallate)	1.58	0.002	0.05	0.002	0.10
M5	5-Hydroxytetradecanedioic acid	1.07	0.009	1.60	0.002	2.36
M6	Quercetin 3-*O*-glucoside	1.57	0.002	1.32	0.002	1.60
M7	Hexadecasphingosine	1.22	0.035	0.84	0.002	0.75
M8	*N*,*N*-Dimethyldodecylamine	1.38	0.002	0.49	0.002	0.53
M9	Sphinganine	1.42	0.003	0.77	0.003	0.76
M10	Dehydrated dyphylline-Glc-C18:3	1.68	0.002	0.06	0.002	0.15
M11	PA (i-14:0/i-13:0)	1.54	0.002	46.83	0.002	267.57
M12	LysoPC (20:5/0:0)	1.63	0.002	—	0.002	—
M13	DG (PGF1alpha/0:0/i-13:0)	1.06	0.035	0.59	0.035	0.58
M14	PGP (20:4-3OH/22:6)	1.01	0.048	1.64	0.002	2.68
M15	PA (22:4/PGF1alpha)	1.61	0.004	0.17	0.003	0.21
M16	Cer (d18:0/12:0)	1.09	0.009	0.52	0.006	0.32
M17	PGP (PGF1alpha/i-22:0)	1.59	0.002	0.07	0.003	0.35
M18	PGP (22:6-2OH/i-22:0)	1.62	0.002	0.06	0.004	0.21
M19	22-Acetylpriverogenin B	1.35	0.013	0.50	0.018	1.77
M20	PGP (TXB2/i-20:0)	1.65	0.002	0.07	0.002	0.24
M21	PGP (20:3-2OH/i-22:0)	1.60	0.002	0.06	0.003	0.19
M22	PA (20:3-OH/22:5)	1.63	0.002	0.09	0.002	0.25
M23	PI (20:3-O/20:0)	1.65	0.002	0.15	0.002	0.44
M24	Cer (d18:0/20:0)	1.13	0.018	0.50	0.006	0.46
M25	SM (d17:1/20:4-2OH)	1.60	0.002	0.23	0.013	0.66
M26	PG (i-14:0/i-13:0)	1.45	0.009	0.64	0.048	0.69
M27	1,2-Di-octadecatrienoyl-3-(galactosyl-alpha-1-6-galactosyl-beta-1)-glycerol	1.62	0.002	0.29	0.002	0.58
M28	PA (22:5/20:2)	1.62	0.025	0.15	0.025	0.50
M29	PC (36:6)	1.59	0.002	0.14	0.009	0.50
M30	14-Hydroxylanosterol	1.48	0.048	0.43	0.035	—

[a] "UF0", "UF10", and "AC10" represent the TELNs isolated from tea leaves at 0 days (unfermented), 10 days (unfermented), and 10 days (AC-fermented), respectively. AC, *Aspergillus cristatus*. "/": Metabolites in one group were not detected.

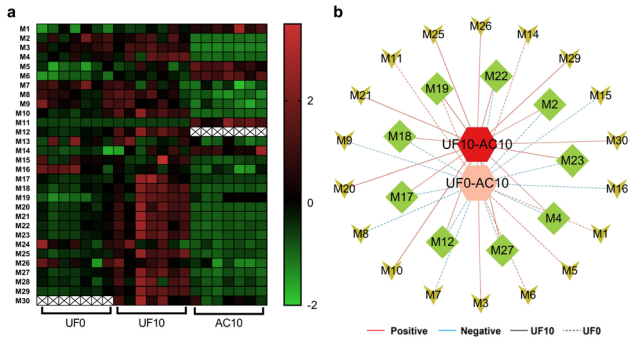

Fig. 4 Heatmap and correlation analysis (a) the relative contents of 30 differential metabolites in the UF0, UF10, and AC10 groups. The value of each compound was the result of *Z*-score transformation of its relative content. The metabolites not detected or had been below the detection limit in the corresponding sample were marked as " × " in the heatmap (b) correlation analysis between the contents of differential metabolites and the particles number of TELNs, $|r| > 0.6$, $p < 0.05$. Solid lines indicate significant correlations between metabolite relative abundance and particle number for the UF10 *vs.* AC10 group comparison; dashed lines indicate significant correlations for the UF0 *vs.* AC10 group comparison; red denotes a positive correlation and blue denotes a negative correlation. "UF0", "UF10", and "AC10" represent the TELNs isolated from tea leaves at 0 days (unfermented), 10 days (unfermented), and 10 days (AC-fermented), respectively. AC, *Aspergillus cristatus*.

Mann–Whitney *U* test ($p < 0.05$). As a result, 30 significantly altered metabolites associated with fermentation were tentatively identified and classified as differential metabolites. The statistical parameters like VIP, *p*-values, and FC of these differential metabolites were summarized in Table 1. Additionally, detailed identification information, including metabolite serial numbers, retention time (RT), accurate mass data (*m*/*z*), molecular formula, mass error, adduct types, and MS/MS spectra, was compiled in SI Table S1.

3.3 Differential metabolites of TELNs

The 30 differential metabolites were classified into four classes: 2 alkaloids, 4 flavonoids, 21 lipids and 3 others. To visualize the intergroup variations in metabolite abundance, heatmaps were generated following *z*-score normalization of the data, as depicted in Fig. 4a. Comparative analysis indicated that the majority of metabolites in fermented TELNs were downregulated compared to those in the unfermented TELNs. Only five metabolites showed upregulated expression, namely M1 (Caffeine), M5 (5-hydroxytetradecanedioic acid), M6 (Quercetin 3-O-glucoside), M11 (PA(i-14:0/i-13:0)) and M14 (PGP (20:4-3OH/22:6)). Interestingly, it was observed that the levels of M19 (22-acetylpriverogenin B) and M30 (14-hydroxylanosterol) increased in the UF10 control group but decreased after AC fermentation, which suggested that AC fermentation might stabilize these compounds during storage.

Spearman's correlation analysis was performed to assess associations between differential metabolites and TELNs particle counts (Fig. 4b). Significant positive correlations ($r > 0.6$, $p < 0.05$) were observed for 17 metabolites in the UF10 group when compared with AC10 controls. In contrast, the UF0

Table 2 Parameters of NAFLD mice treated with TELNs for 4 weeks (mean ± SD, $n = 8$).[a]

Group	TC (mmol L^{-1})	TG (mmol L^{-1})	HDL-C (mmol L^{-1})	LDL-C (mmol L^{-1})	AI	ALT (U L^{-1})	AST (U L^{-1})	IL-6 (pg mL^{-1})	TNF-α (pg mL^{-1})
N	3.38 ± 0.25***	0.61 ± 0.07***	2.60 ± 0.43***	0.44 ± 0.10***	0.32 ± 0.20*	13.55 ± 1.23**	13.70 ± 2.97**	9.05 ± 3.30 ***	26.75 ± 3.15***
M	6.04 ± 0.86	0.78 ± 0.04	3.75 ± 0.34	0.91 ± 0.22	0.62 ± 0.25	16.72 ± 1.59	21.98 ± 3.94	32.23 ± 5.69	100.59 ± 26.04
P	4.97 ± 0.65*	0.72 ± 0.15	2.86 ± 0.51**	0.89 ± 0.16	0.78 ± 0.32	13.92 ± 1.80**	13.89 ± 2.81**	15.19 ± 6.54**	84.55 ± 11.03
UF	4.62 ± 0.61**	0.73 ± 0.23	3.17 ± 0.42**	0.95 ± 0.19	0.46 ± 0.13	14.00 ± 2.39*	14.92 ± 2.23**	15.16 ± 3.29***	49.48 ± 4.90***
AC	4.03 ± 0.31***#	0.62 ± 0.13*	3.29 ± 0.35*	0.68 ± 0.10*##	0.24 ± 0.14*##	13.40 ± 2.60*	13.74 ± 3.98**	10.27 ± 3.69***#	42.53 ± 6.12***#

[a] Mann–Whitney *U* test was used to calculate significant difference. $^{*}p < 0.05$, $^{**}p < 0.01$, $^{***}p < 0.001$, compared with M group; $^{\#}p < 0.05$, $^{\#\#}p < 0.01$, AC group compared with UF group N: normal group; M: NAFLD model group; P: positive group; UF: UF0 treatment group; AC: AC10 treatment group. "UF0" and "AC10" represent the TELNs isolated from tea leaves at 0 days (unfermented) and 10 days (AC-fermented), respectively. AC, *Aspergillus cristatus*.

group displayed positive correlations with 6 metabolites and negative correlations with 13 metabolites. Among these, 9 metabolites showed significant correlations with TELNs particle counts both before and after fermentation. Notably, the concentration of M19 (22-acetylpriverogenin B) demonstrated a progressive increase with elevated TELNs particle counts. These findings indicated that TELNs abundance significantly influenced metabolite concentration, with all reported correlations satisfying the strict statistical criteria ($|r| > 0.6$, $p < 0.05$).

3.4 Preventive effect of TELNs against NAFLD

The lipid-modulating effects of TELNs in HFD-induced NAFLD mice were systematically evaluated. Key parameters such as TC, TG, HDL-C, LDL-C, AI, ALT, AST, IL-6 and TNF-α were summarized in Table 2. After the 6-week experimental period, significant alterations in TC, TG, HDL-C, LDL-C, AI, ALT, AST, IL-6 and TNF-α were observed in HFD-fed mice when compared to the N group. The combination of these metabolic alterations with hepatic morphological and histopathological assessments confirmed the successful establishment of the NAFLD model. Notably, all treatment groups exhibited significant reductions in serum TC, HDL-C, ALT, AST, IL-6 and TNF-α levels compared to the M group. The AC group demonstrated substantial improvements, with significantly decreased TG, LDL-C and AI values. Moreover, the AC group displayed superior lipid-lowering efficacy than the UF group, as evidenced by significantly lower TC, LDL-C, AI, IL-6 and TNF-α levels ($p < 0.05$).

Following 6 weeks of high-fat diet intervention, the results of body weight and liver weight in mice were shown in Fig. 5c and d. Mice in the high-fat model group exhibited a significant increase in body weight, while their liver weight showed minimal changes. The hepatoprotective effects of TELNs before and after fermentation were evaluated through comprehensive morphological and histopathological analyses of mouse liver tissues. As demonstrated in Fig. 5a, livers from HFD-fed mice exhibited characteristic steatotic features, including oily texture and slightly grayish-white discoloration after 6 weeks. The oil red O staining results presented in Fig. 5b clearly demonstrated distinct pathological disparities. In the N group, the hepatic architecture remained normal, characterized by hepatocytes radially distributed around central veins. Conversely, in the M group, there was conspicuous lipid droplet accumulation, as indicated by the red staining. Additionally, nuclear displacement and widespread vacuolization were observed. Notably, following 4 weeks of treatment, all intervention groups showed varying degrees of histological improvement, with a particularly significant reduction in lipid droplet accumulation, and the quantitative results of liver lipids were shown in Fig. 5e. Collectively, these findings demonstrated that AC-fermented TELNs were more effective than unfermented counterparts in attenuating hepatic steatosis, reducing lipid accumulation and alleviating inflammation in HFD-induced NAFLD mice.

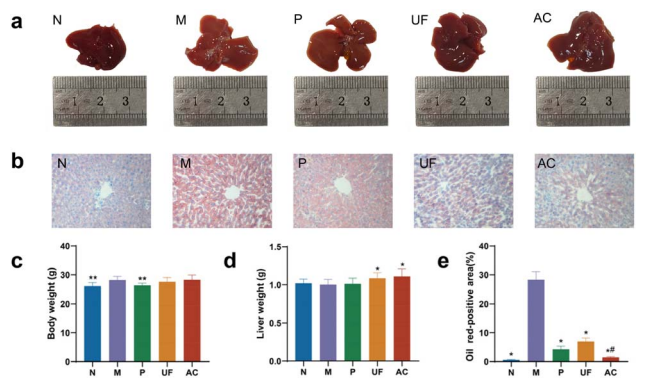

Fig. 5 The effect of each group on the histopathology of liver tissue. (a) Liver morphology (b) representative photomicrograph of liver histology (oil red-O staining, magnification 100×) (c) body weight (d) liver weight (e) oil O red-positive area. *$p < 0.05$, **$p < 0.01$, compared with M group; $^{\#}p < 0.05$, AC group compared with UF group. N: normal group; M: NAFLD model group; P: positive group; UF: UF0 treatment group; AC: AC10 treatment group. "UF0" and "AC10" represent the TELNs isolated from tea leaves at 0 days (unfermented) and 10 days (AC-fermented), respectively. AC, *Aspergillus cristatus*.

4. Discussion

In this study, TELNs were successfully isolated from dark tea. Subsequently, a comprehensive comparative analysis of their physical characteristics, compositional profiles, and functional properties was conducted for the first time to investigate the effects of fermentation on TELNs. Systematic evaluation revealed that AC fermentation significantly reduced TELNs' particle size, enhanced their secretion yield, modified their biochemical composition, and improved their lipid-lowering and anti-inflammatory efficacy against NAFLD.

The experimental results demonstrated significant alterations in the physicochemical properties of TELNs following AC fermentation. The observed reduction in TELNs particle size after fermentation likely resulted from two possible reasons: the integration of smaller fungal-derived extracellular vesicles with the native TELNs;[3,29] and structural compaction induced by increased polysaccharide coating on TELNs surfaces during fermentation.[21,30] Concurrently, fermentation enhanced TELNs secretion likely *via* activated interkingdom communication between plant cells and fermenting microorganisms. This phenomenon was supported by evidence that microbial stimulation induced increased production of PELNs that served as molecular messengers, accumulating at interaction sites and being taken up by fungal cells.[31,32] Interestingly, the control group UF10 showed increased TELNs levels during storage. This might be related to the metabolite accumulation caused by degradation, aggregation, and auto-oxidation processes, which subsequently triggered exosome-mediated material transport.[33] In contrast, the fermented group AC10 showed reduced secretion compared to UF10. This was possibly because TELNs loaded with multiple active components might be consumed as nutrients for fungal growth. In addition, the change in protein content might be jointly associated with the number of TELNs particles and the protein loading efficiency within the particles, and that the specific regulatory mechanism required further analysis.[34]

The differential metabolites in TELNs before and after AC fermentation were predominantly concentrated in alkaloids, flavonoids, and lipids, which were consistent with our previous study.[12] Existing literature had demonstrated that caffeine exhibited notable neuro-stimulatory activity, and the health benefits of dark tea were enhanced through the modulation of the central nervous system.[35] Moreover, theophylline could be converted into caffeine by *Aspergillus* spp.[36] Among flavonoids, catechins such as Epicatechin 3-*O*-gallate could be transformed into pigment substances by microbial oxidase activity.[37] This transformation contributed to the characteristic brown-red infusion of dark tea. Flavonol glycosides, like Quercetin-3-*O*-glucoside, could be derived from rutin *via* glycosidase hydrolysis, imparting a velvety smoothness at minuscule threshold concentrations.[38,39] The findings of our study on TELNs were consistent with relevant literature regarding dark tea fermentation.

Additionally, significant alterations were observed in approximately 70% of lipids within the TELNs metabolite profile following fermentation, with phospholipid species demonstrating particularly pronounced abundance changes. Notably, M11 (PA(i-14:0/i-13:0)) exhibited a 267.67-fold increase after fermentation, representing the most substantial change observed. This phenomenon may be attributed to complex interactions between glycerophospholipids and fungal growth and metabolic activities.[40,41] Concurrently, two triterpenoid compounds (M19 and M30) both showed reduced accumulation during storage following AC fermentation, further supporting the involvement of lipids in fungal biological processes.[42] Moreover, a Spearman correlation analysis was performed between differential metabolite concentrations and TELNs particle counts based on metabolomics research method. Significant correlations were identified between 9 differential metabolites and TELNs particle number variations during fermentation. These findings not only demonstrated the central regulatory role of TELNs in modulating differential metabolite expression but also suggested that fermentation could indirectly influence metabolite profiles by altering the concentration or functional properties of TELNs. Collectively, these results confirmed substantial compositional changes in TELNs-associated metabolites during the fermentation process.

Previous studies have demonstrated that Fu brick tea fermented with AC could ameliorate HFD-induced insulin resistance, hepatic steatosis, and inflammation in mice.[11,13] Similarly, extracellular vesicles isolated from fresh tea leaf homogenates were shown to significantly attenuate CCl4-induced liver fibrosis and reduce lipid droplet accumulation in hepatic tissue.[43] These findings collectively suggested that dark tea-derived TELNs possess the potential to improve NAFLD. Based on this evidence, a NAFLD mouse model was employed to investigate functional alterations in TELNs before and after fermentation. Our experimental results supported this hypothesis, revealing that dark tea-derived TELNs effectively regulated blood lipid levels and reduced hepatic lipid accumulation in NAFLD mice. Notably, fermented TELNs exhibited a 10% greater lipid-lowering efficacy compared to their unfermented counterparts. Beyond these tea-related observations, in recent years, extracellular vesicle-based therapeutic strategies have emerged as a new frontier in the study of metabolic diseases.[44] Multiple studies have demonstrated that plant-derived vesicle-like nanoparticles, such as those isolated from honey and garlic chives, alleviated hepatic inflammation and fibrosis by inhibiting the NLRP3 inflammasome and NF-κB pathways.[45,46] Meanwhile, apical papilla stem cell-derived exosomes were shown to ameliorate NASH by promoting macrophage polarization toward the M2 phenotype.[47] A central mechanism underlying the hepatoprotective effects of these interventions involved the suppression of key inflammatory signaling pathways, including NF-κB and NLRP3, leading to a marked reduction in the levels of downstream effector cytokines such as TNF-α and IL-6. Consistent with these findings, the present study observed that treatment with TELNs significantly reduced the expression of TNF-α and IL-6 in a NAFLD mouse model, suggesting that TELNs likely ameliorate NAFLD through a similar anti-inflammatory mechanism mediated by the inhibition of critical inflammatory pathways.

Furthermore, existing literature had reported hepatoprotective effects of fungi and fungal-derived extracellular vesicles. For example, *Eurotium cristatum* particle metabolites could enhance hepatic detoxification through PXR and AhR pathways,[48] and shiitake mushroom-derived ELNs (S-ELNs) could inhibit fulminant hepatic failure by suppressing the NLRP3 inflammasome.[49] These observations suggested that the protective effects of TELNs against NAFLD were not limited to tea-derived TELNs alone. It was highly possible that fungal nanovesicles were also involved in exerting pharmacological effects or had a synergistic effect with tea-derived TELNs to jointly intervene in NAFLD. However, further direct investigation was required to demonstrate this inference.

5. Conclusion

In summary, this study used a combination of differential centrifugation and SEC to isolate TELNs from decoction before and after fermentation of dark tea, and conducted a comprehensive analysis of the difference of TELNs before and after fermentation of tea. It was found that AC fermentation significantly reduced the average particle size of TELNs, increased secretion of TELNs, and altered the expression levels of key metabolites such as flavonoids, alkaloids, and lipids. Furthermore, AC fermentation enhanced the lipid-lowering and anti-inflammatory efficacy of TELNs in NAFLD mice. This study provided valuable insights into the molecular-level changes of tea leaves after microbial fermentation and also offered a new perspective for the applications of dark tea and TELNs in fields such as food science, medicine, and healthcare.

Ethical statement

All animal experiments were approved by the Institutional Animal Care and Use Committee of Hubei University of Chinese Medicine (Approval No. HUCMS 78475747), and were carried out in compliance with all relevant ethical regulations.

Author contributions

Meiling Guo: conceptualization, methodology, data curation, formal analysis and investigation, visualization, writing – original draft; Chengwu Song: conceptualization, methodology, writing – review & editing, funding acquisition; Jing Tang: methodology, data curation, writing – review & editing, resources; Yiping Li: formal analysis and investigation, software, visualization; Zhaoxiang Zeng: formal analysis and investigation, software; Xiaoliu Hu: formal analysis and investigation, validation; Xin Huang: data curation, resources; Sha Wei: data curation, resources; Cheng Chen: data curation, resources; Yinping Tang: writing – review & editing, project administration, supervision; Rongzeng Huang: conceptualization, writing – review & editing, project administration; Shuna Jin: methodology, writing – original draft, funding acquisition, project administration, supervision.

Conflicts of interest

There are no conflicts to declare.

Data availability

The data supporting this article have been included as part of the SI, including MS-DIAL parameter settings, Fig. S1: PCA score scatter plots, and Table S1: Identification results of differential metabolites. See DOI: **https://doi.org/10.1039/d5ra03044g**.

Acknowledgements

This research was funded by the Science Foundation of Hubei Provincial Department of Education (No. D20222003) and the projects of the Hubei University of Chinese Medicine (No. 2023ZZXJ001 and No. 2022ZZXT003).

References

1 Q. Gao, N. Chen, B. Li, M. Zu, Y. Ma, H. Xu, Z. Zhu, R. L. Reis, S. C. Kundu and B. Xiao, *J. Nanobiotechnol.*, 2024, **22**, 4.
2 L. Yan, Y. Cao, L. Hou, T. Luo, M. Li, S. Gao, L. Wang, K. Sheng and L. Zheng, *J. Adv. Res.*, 2024, 1–15, DOI: **10.1016/j.jare.2024.04.001**.
3 M. Zu, D. Xie, B. S. B. Canup, N. Chen, Y. Wang, R. Sun, Z. Zhang, Y. Fu, F. Dai and B. Xiao, *Biomaterials*, 2021, **279**, 121178.
4 H. A. Dad, T. W. Gu, A. Q. Zhu, L. Q. Huang and L. H. Peng, *Mol. Ther.*, 2021, **29**, 13–31.
5 Q. Chen, M. Zu, H. Gong, Y. Ma, J. Sun, S. Ran, X. Shi, J. Zhang and B. Xiao, *J. Nanobiotechnol.*, 2023, **21**, 6.
6 M. Xu, L. Ma, H. Liang, W. Tang and S. Gu, *Front. Pharmacol*, 2024, **15**, 1476820.
7 J. Zou, Q. Song, P. C. Shaw, Y. Wu, Z. Zuo and R. Yu, *Int. J. Nanomed.*, 2024, **19**, 10023–10043.
8 B. Wang, X. Zhuang, Z. B. Deng, H. Jiang, J. Mu, Q. Wang, X. Xiang, H. Guo, L. Zhang, G. Dryden, J. Yan, D. Miller and H. G. Zhang, *Mol. Ther.*, 2014, **22**, 522–534.
9 Y. Liu, D. Cao, L. Ma and X. Jin, *Plant Physiol. Biochem.*, 2022, **183**, 138–150.
10 G. Chen, G. Zhu, H. Xie, J. Zhang, J. Huang, Z. Liu and C. Wang, *Food Res. Int.*, 2024, **194**, 114928.
11 B. Li, Q. Mao, R. Xiong, D. Zhou, S. Huang, A. Saimaiti, A. Shang, M. Luo, H. Li, H. Li and S. Li, *Foods*, 2022, **11**, 3457.
12 Z. Zeng, S. Jin, X. Xiang, H. Yuan, Y. Jin, Q. Shi, Y. Zhang, M. Yang, L. Zhang, R. Huang and C. Song, *Food Res. Int.*, 2023, **170**, 112992.
13 Z. Lu, Y. Zheng, J. Zheng, Q. Liang, Q. Zhen, M. Cui, H. Yang, H. Wu, C. Tian, K. Zhu, C. Bian, L. Du, H. Wu and X. Guo, *Food Funct.*, 2024, **15**, 4421–4435.
14 J. Wan, M. Feng, W. Pan, X. Zheng, X. Xie, B. Hu, C. Teng, Y. Wang, Z. Liu, J. Wu and S. Cai, *Antioxidants*, 2021, **10**, 1513.
15 X. Xiang, Y. Xiang, S. Jin, Z. Wang, Y. Xu, C. Su, Q. Shi, C. Chen, Q. Yu and C. Song, *J. Food Sci.*, 2020, **85**, 2933–2942.
16 Y. K. Liu, X. L. Xiang, Z. X. Zeng, M. L. Guo, Y. P. Li, Z. C. Zhan, R. Z. Huang, M. Zhao, S. A. Jin and C. W. Song, *Int. J. Food Sci. Technol.*, 2024, **59**, 5398–5410.
17 X. Xiang, C. Su, Q. Shi, J. Wu, Z. Zeng, L. Zhang, S. Jin, R. Huang, T. Gao and C. Song, *Food Funct.*, 2021, **12**, 7546–7556.
18 F. J. Lin, X. L. Wei, H. Y. Liu, H. Li, Y. Xia, D. T. Wu, P. Z. Zhang, G. R. Gandhi, H. B. Li and R. Y. Gan, *Trends Food Sci. Technol.*, 2021, **109**, 126–138.
19 H. P. Lv, Y. Zhang, J. Shi and Z. Lin, *Food Res. Int.*, 2017, **100**, 486–493.
20 C. Guo, W. Shen, W. Jin, X. Jia, Z. Ji, J. Li and B. Li, *J. Food Sci.*, 2023, **88**, 4068–4078.
21 R. Zhu, Z. Chen, H. Lv, Y. Pan, X. Feng, G. Chen, W. Hu, T. Xu, F. Fan, S. Gong, P. Chen and Q. Chu, *Food Chem.*, 2023, **429**, 136838.
22 H. Han, L. Ke, W. Xu, H. Wang, J. Zhou and P. Rao, *Food Funct.*, 2023, **14**, 8420–8430.
23 X. Lei, H. Li, S. Chen, B. Li, H. Xia, J. Li, F. Guan and J. Ge, *Bioresour. Bioprocess.*, 2025, **12**, 9.
24 H. Han, L. J. Ke, H. Q. Wang, G. Z. Gao, Y. Zhang, P. F. Rao, J. W. Zhou, O. Tirosh and B. Schwartz, *Food Biophys.*, 2022, **17**, 209–220.
25 X. Li, Z. Liang, J. Du, Z. Wang, S. Mei, Z. Li, Y. Zhao, D. Zhao, Y. Ma, J. Ye, J. Xu, Y. Zhao, J. Chang, Y. Qin, L. Yu, C. Wang and C. Jiang, *Sci. China:Life Sci.*, 2019, **62**, 333–348.
26 Q. Shi, S. Jin, X. Xiang, J. Tian, R. Huang, S. Li, C. Chen, H. Xu and C. Song, *Food Funct.*, 2019, **10**, 7782–7792.
27 J. Wei, Z. Zeng, C. Song, Q. Lv, G. Chen, G. Mo, L. Gong, S. Jin, R. Huang and B. Huang, *Front. Plant Sci.*, 2024, **15**, 1498577.
28 J. Y. You, S. J. Kang and W. J. Rhee, *Bioact. Mater.*, 2021, **6**, 4321–4332.
29 V. S. Brauer, A. M. Pessoni, T. A. Bitencourt, R. G. de Paula, L. D. Rocha, G. H. Goldman and F. Almeida, *Msphere*, 2020, **5**, 00190.
30 Q. Li, L. Liu, J. Zhang, M. Dong, L. Wang, D. Julian McClements, Y. Fu, L. Han, P. Shen and X. Chen, *Food Chem.*, 2023, **410**, 135353.

31 Q. Cai, L. Qiao, M. Wang, B. He, F. M. Lin, J. Palmquist, S. D. Huang and H. Jin, *Science*, 2018, **360**, 1126–1129.
32 B. D. Rutter and R. W. Innes, *Plant Physiol.*, 2017, **173**, 728–741.
33 H. Lv, X. Feng, H. Song, S. Ma, Z. Hao, H. Hu, Y. Yang, Y. Pan, S. Zhou, F. Fan, S. Gong, Q. Chu and P. Chen, *Trends Food Sci. Technol.*, 2023, **140**, 104172.
34 A. Steć, M. Chodkowska, J. Kasprzyk-Pochopień, P. Mielczarek, W. Piekoszewski, B. Lewczuk, A. Płoska, L. Kalinowski, B. Wielgomas and S. Dziomba, *Food Chem.*, 2023, **424**, 136333.
35 S. Camandola, N. Plick and M. P. Mattson, *Neurochem. Res.*, 2019, **44**, 214–227.
36 X. Wang, X. Wan, S. Hu and C. Pan, *Food Chem.*, 2008, **107**, 1086–1091.
37 S. Wang, Y. Qiu, R. Y. Gan and F. Zhu, *Food Res. Int.*, 2022, **154**, 110899.
38 H. J. You, H. J. Ahn and G. E. Ji, *J. Agric. Food Chem.*, 2010, **58**, 10886–10892.
39 S. Scharbert, N. Holzmann and T. Hofmann, *J. Agric. Food Chem.*, 2004, **52**, 3498–3508.
40 B. Zhang, J. Zhou, Q. Li, B. Gan, W. Peng, X. Zhang, W. Tan, L. Jiang and X. Li, *PeerJ*, 2019, **7**, e6846.
41 K. K. Mahto, A. Singh, N. K. Khandelwal, N. Bhardwaj, J. Jha and R. Prasad, *PLoS One*, 2014, **9**, e113664.
42 C. You, D. Qin, Y. Wang, W. Lan, Y. Li, B. Yu, Y. Peng, J. Xu and J. Dong, *J. Fungi*, 2021, **7**(10), 788.
43 Q. Gong, Z. Zeng, T. Jiang, X. Bai, C. Pu, Y. Hao and Y. Guo, *Front. Nutr.*, 2022, **9**, 1009139.
44 A. D. P. Abreo Medina, M. Shi, Y. Wang, Z. Wang, K. Huang and Y. Liu, *J. Agric. Food Chem.*, 2025, 2717–2731, DOI: **10.1021/acs.jafc.4c09209**.
45 B. Liu, P. L. Nguyen, H. Yu, X. Li, H. Wang, T. G. B. Nguyen, P. K. Sahoo, M. Sur, J. Reddy, S. Sillman, S. D. Kachman, B. Altartouri, G. Lu, S. K. Natarajan, M. Pattabiraman and J. Yu, *Acta Pharm. Sin. B*, 2024, **14**, 3661–3679.
46 B. Liu, X. Li, H. Yu, X. Shi, Y. Zhou, S. Alvarez, M. J. Naldrett, S. D. Kachman, S. H. Ro, X. Sun, S. Chung, L. Jing and J. Yu, *Theranostics*, 2021, **11**, 9311–9330.
47 Y. Nie, W. Meng, D. Liu, Z. Yang, W. Wang, H. Ren, K. Mao, W. Lan, C. Li, Z. Wang and J. Lan, *Mol. Med.*, 2024, **30**, 186.
48 X. X. Huang, S. Xu, L. J. Yu, Y. F. Zhou, Y. Zhou and Z. H. Liu, *Oxid. Med. Cell. Longevity*, 2021, **2021**, 6635080.
49 B. L. Liu, Y. Z. Lu, X. Y. Chen, P. G. Muthuraj, X. Z. Li, M. Pattabiraman, J. Zempleni, S. D. Kachman, S. K. Natarajan and J. J. Yu, *Nutrients*, 2020, **12**, 477.